CRITICAL EVALUATION AND THERMODYNAMIC MODELING OF SELECTED COPPER BASED BINARY ALLOYS

D. J. Chakrabarti
Alcoa Laboratories
Alcoa Center, PA 15069
USA

and

D. E. Laughlin
Carnegie -Mellon University
Pittsburgh, PA 15213
USA

Summary

The relationship between the thermodynamic properties of alloys and their phase equilibria can be utilized for the critical evaluation of binary systems. We show how limited experimental thermodynamic data can be used to derive the most likely phase boundaries in systems with conflicting reports. In cases where no thermodynamic data are available, the known phase diagrams can be utilized for thermodynamic modeling to derive parameters for the different phases, which in turn can reproduce the phase diagram consistently. Comparisons of these parameters with known experimental data often indicate reasonably good agreement. Using these parameters the phase equilibria in unreported regions of the phase diagram can be predicted. These features are exemplified in this review using case studies from the Cu-Cr, Cu-Th, Cu-Ca, Cu-Sr and Cu-Ir systems.

Introduction

The phase diagram and the thermodynamic properties of the corresponding phases are closely interrelated. If Gibbs energy changes with temperature and composition are known for the different phases, then from the common tangent construction the phases coexisting with each other, and the corresponding equilibrium compositions can be ascertained. Thus, if adequate and reliable thermodynamic data are available, they can be utilized directly to calculate the phase diagram.

Both phase diagram and thermodynamic property determinations require utmost care to ensure that equilibrium is maintained. Inaccuracies and contradictions abound in the literature. Experimental data are comparatively more abundant on phase diagrams than on thermodynamic properties, owing to the earlier development of interest in the former and the relative ease in their measurement. Thermodynamic data are useful more often to confirm or to resolve contradictions between different reported phase diagrams, than for their direct calculation. Where accurate data are available, however, they can be utilized to model regions of phase diagrams which are experimentally difficult to determine, such as at extremely high or low temperatures. The data can also be used to determine metastable phase boundaries and extensions of equilibrium phase boundaries into metastable regions. Conversely, phase diagrams can be utilized to derive thermodynamic parameters for the related phases, either as a source of primary data, or for comparison with experimental thermodynamic results. These thermodynamic parameters can also be used to calculate unknown regions of the phase diagram.

Modeling of equilibrium between coexisting phases requires knowledge of the Gibbs energy for each of the phases. For a phase ß, formed from the components A and B, the Gibbs energy, G, can be expressed as follows:

$$G^{\beta} = [(1-X)G_A^{\beta} + XG_B^{\beta}] + [RT(X\ln X+(1-X)\ln(1-X))] + [\Delta H - T^{E}\Delta S] \quad (1)$$

where, G_A^{β} and G_B^{β} are Gibbs energies for components A and B in the ß phase, ΔH and $^{E}\Delta S$ are the enthalpy and excess entropy of formation of the ß phase from components A and B, R is the gas constant and X is the atomic fraction of B. The Gibbs energy expression within the first pair of brackets refers to that for a mechanical mixture of A and B, within the second pair to that due to the configurational entropy, while the term $[\Delta H - T^{E}\Delta S]$ refers to the excess free energy for the formation of the ß phase. Thus to define the Gibbs energy of a phase, knowledge of the excess free energy, $^{E}\Delta G$, term is essential. In this review, both ΔH and $^{E}\Delta S$ terms are represented as polynomials with composition as follows:

$$\Delta H = X(1-X) \sum_{i=1}^{N} a_i X^{i-1} \qquad (2)$$

$$E_{\Delta S} = X(1-X) \sum_{j=1}^{N} b_j X^{j-1} \qquad (3)$$

Some solution models in use in the increasing order of their complexity are :

(1) Ideal Solution : all a_i and b_j parameters are equal to zero.

(2) Regular Solution : a_1 = constant ; all other a_i and b_j = 0.

(3) Subregular Solution : a_1 = constant, a_2 = constant ; all other a_i and b_j = 0.

A more generalized expression for the solution is where one or more terms of both a_i and b_j's are non-zero. Herein, it is assumed that the Kopp-Neumann rule holds, in that the coefficients a_i and b_j are temperature independent.

The values for the coefficients a_i and b_j are normally obtained by fitting Eqs 2 and 3 to experimentally determined ΔH values and to the derived (from ΔH and ΔG values) ΔS values. Where such data do not exist or are restricted, we instead use the known phase diagrams as a source. This is done based on the well-known principle of the equality of chemical potentials of phases at equilibrium.

$$\mu_A^{\alpha}(X_\alpha) = \mu_A^{\beta}(X_\beta) \qquad (4)$$

$$\mu_B^{\alpha}(X_\alpha) = \mu_B^{\beta}(X_\beta) \qquad (5)$$

where, X_α and X_β are the compositions of α and β phases coexisting with each other at the temperature T.

Combining Eqs 1 to 4 for component A, we obtain :

$$\sum_{i=0}^{Na} [(i+1)X_\alpha^{i+2} - iX_\alpha^{i+1}]\, a_i^{\alpha} - T \sum_{j=0}^{Pa} [(j+1)X_\alpha^{j+2} - jX_\alpha^{j+1}]\, b_j^{\alpha}$$

$$- \sum_{i=0}^{N_\beta} [(i+1)X_\beta^{i+2} - iX_\beta^{i+1}]\, a_i^\beta + T \sum_{j=0}^{P_\beta} [(j+1)X_\beta^{j+2} - jX_\beta^{j+1}]\, b_j^\beta$$

$$= (G_A^\beta - G_A^a) + RT \ln[(1-X_\beta)/(1-X_a)] \qquad (6)$$

Likewise, combining Eqs 1 to 3 and 5 for component B, we obtain:

$$\sum_{i=0}^{Na} [(i+1)(X_a^{i+2} - 2X_a^{i+1} + X_a^i)]\, a_i^a - T \sum_{j=0}^{Pa} [(j+1)(X_a^{j+2} - 2X_a^{j+1} + X_a^j)]\, b_j^a$$

$$-\sum_{i=0}^{N\beta} [(i+1)(X_\beta^{i+2} - 2X_\beta^{i+1} + X_\beta^i)]\, a_i^\beta + T \sum_{j=0}^{P\beta} [(j+1)(X_\beta^{j+2} - 2X_\beta^{j+1} + X_\beta^j)]\, b_j^\beta$$

$$= (G_B^\beta - G_B^a) + RT \ln(X_\beta/X_a) \qquad (7)$$

Equations 6 and 7 can be solved for the unknown coefficients a_i and b_j from the requisite number of tie-line data points, and from the known values of the lattice stability parameters.

In what follows, four examples of the application of the above approaches in modeling phase diagrams will be presented. These are :

Case A - The utilization of thermodynamic data to resolve a controversy (Cu-Cr phase diagram),

Case B - A demonstration that modeling parameters obtained from phase diagrams in Eqs 6 and 7 are often realistic, and compare well with measured values, (Cu-Th and Cu-Ca systems),

Case C - A demonstration that the parameters are not only self-consistent in that they reproduce the original phase diagram satisfactorily, but also that they can be utilized to predict unknown phase reactions, (Cu-Sr system),

Case D - An illustration of how the parameters derived from known regions of the phase diagram can be utilized in calculating either other parts of the diagram, which are difficult to determine experimentally, or metastable phase boundaries, (Cu-Ir system).

Case A

The Cu-Cr equilibrium diagram is indicated in the literature (1, 2) as having a large miscibility gap in the liquid above 1467°C. The conclusion is, however, based on limited data, obtained on specimens that had large impurity contents (3, 4). A preliminary calculation of the liquidus by Kuznetsov, Fedorov and Rodnyanskaya (5) showed the occurrence of a flat (nearly horizontal) liquidus, and not a miscibility gap. The calculations were based on interaction parameters for the liquid that were derived from phase equilibria data at 1150 to 1330°C between the liquid and the (Cr) phase. Activity measurements between 1402 and 1616°C by Timberg and Toguri (6), indicated the presence of (Cr) phase in equilibrium with the liquid at 1550°C for compositions above 42 at.% Cr. These observations failed to document the occurrence of a miscibility gap in the liquid.

In our calculation (7), we utilized the thermodynamic data of Timberg et al. (6), and optimized these with the solubility data given by Kuznetsov et al. (5). These gave an expression for the interaction parameter of the liquid that incorporated not only a temperature dependence (5), but also a composition dependence. The following approach was used.

The composition dependence of Cr on the interaction parameter of the liquid, Ω_{Cr}^{l}, was derived from the partial molar excess Gibbs energy values for Cr, $^{E}\Delta\bar{G}_{Cr}^{l}$, obtained from the activity data of Timberg et al. (6). This had the following relationship:

$$\Omega_{Cr}^{l} = 6070X_{Cr} + 33100 \qquad \text{(J/mol)} \qquad (8)$$

The values of Ω_{Cr}^{l} were also calculated from the composition of the liquid in equilibrium with the (Cr) phase, based on the following relation that assumes the solid solution as Raoltian.

$$\Omega_{Cr}^{l} = [\Delta G_{Cr}^{l \rightarrow (Cr)} + RT \ln(X_{Cr}^{(Cr)}/X_{Cr}^{l})] / (1 - X_{Cr}^{l})2 \qquad (9)$$

where, $\Delta G_{Cr}^{l \rightarrow (Cr)} = -16930 + 7.95\,T$ (J/mol) is the Gibbs energy of fusion of Cr (2). The Ω_{Cr}^{l} values were modified to correspond to a fixed composition, namely the eutectic point at $X_{Cr} = 0.0156$, based on the composition dependence given in Eq 8. The resultant expression for Ω_{Cr}^{l}

as a function of both temperature and composition was obtained as:

$$\Omega_{Cr}^{l} = 81200 + 6070\,X_{Cr} - 27.9\,T \qquad \text{(J/mol)} \qquad (10)$$

The interaction parameter values for Cu in the liquid, Ω_{Cu}^{l}, were derived from the above expression for Ω_{Cr}^{l} by the application of the Gibbs-Duhem relation for the temperature dependent part. The composition dependence of Ω_{Cu}^{l} was obtained from the $^{E}\Delta\bar{G}_{Cu}^{l}$ values of Timberg et al. (6). The combined T and X dependence was as follows:

$$\Omega_{Cu}^{l} = 79500 + 6070\,X_{Cr} - 27.9\,T \qquad \text{(J/mol)} \qquad (11)$$

The resultant integral expression for Ω^{l} derived from Eqs. 10 and 11 was:

$$\Omega^{l} = 81200 + 4400\,X_{Cr} - 27.9\,T \qquad \text{(J/mol)} \qquad (12)$$

Based on the above expression for Ω^{l} and assuming a simple Henrian solution for (Cr), the resultant liquidus as well as its metastable miscibility gap at lower temperatures were calculated and are presented in Fig. 1. The Gibbs energies of fusion for Cu and Cr in these calculations were obtained from literature (2).

The calculation demonstrates clearly that the liquid in this system develops a miscibility gap that lies just below the stable liquidus. This accounts for the large flat portion of the liquidus in the mid-composition region. This also explains the several observations of the liquid miscibility gap by early investigators, in that small amounts of impurities may be sufficient to stabilize the gap. The difference between our calculated liquidus and the assessed liquidus from the experimental data (5 & 6), is a consequence of the inherent approximations used in deriving Ω^{l}. However, the general conclusion regarding the proximity of the miscibility gap to the liquidus is expected to be still valid.

This illustrates an example of the use of thermodynamic data to resolve controversies in phase diagram results.

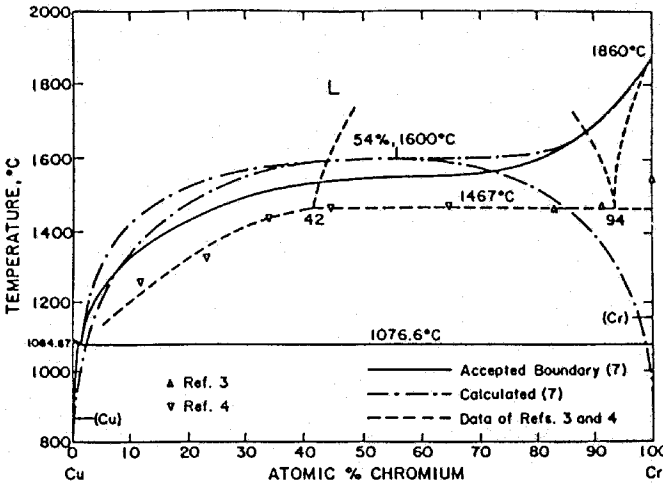

Figure 1 - The Copper-Chromium Phase Diagram. The calculated curves (7) show the stable liquidus and the metastable miscibility gap of the liquid. The accepted liquidus is drawn to conform with experimental results (5 and 6).

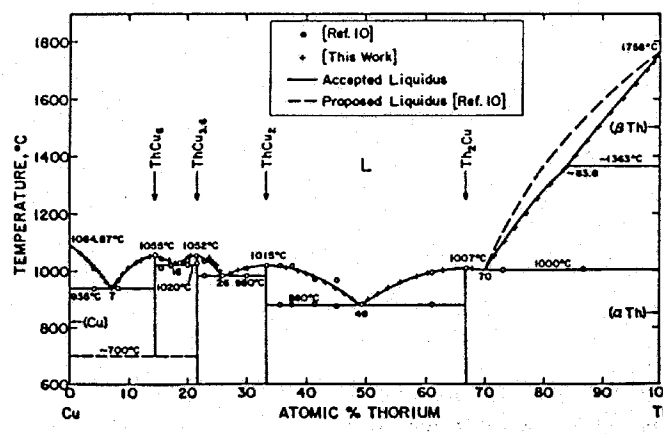

Figure 2 - The Copper-Thorium Phase Diagram. The liquidus data above 70 at.% Th and the eutectoid transformation at ~700°C are based on modeling analysis (9).

The Cu-Th equilibrium diagram is shown in Fig. 2. The enthalpies of formation, ΔH^0, for all the four compounds have been determined experimentally (8), but the same for the liquid is not known. Because both (Cu) and (Th) phases display virtually zero solubility, they are assumed to be line phases, and their molar free energies are represented by the lattice stability parameter values for the solid -> liquid transitions of Cu and Th, respectively, (including the βTh -> αTh transition), see Table I (2).

For the initial analysis (9), liquidus boundaries in equilibrium with (Cu) and (Th), between 1084.87 and 935°C, and between 1758 and 1000°C, respectively, were utilized to derive the parameters for the liquid, applying Eqs 6 and 7. The simultaneous linear equations, set up from the equilibrium between these phases at several temperatures, were solved by the conventional multiple least squares, regression analysis (and the Gauss-Jordan reduction algorithm). The comparison of the derived ΔH^0 and ΔG^0 values for the compounds with those of Bailey and Smith (8), however, showed large discrepency. Apparently, the interpolated liquidus coexisting with (Th), as proposed by Schiltz, Stevens and Carlson (10) in the absence of experimental data, was not correct, and gave inaccurate interaction parameters for the liquid phase.

A modified approach was attempted next. Since the (Cu) and (Th) phases have negligible solubility fields, the limiting slopes for the liquidus in both the instances are given according to van't Hoff's relation:

$$\Delta T / X_i^l = -[R (T_j^m)^2] / \Delta H_j^{s \rightarrow l} \qquad (13)$$

In this equation, $\Delta T / X_i^l$ is the limiting slope of the liquidus for the solute X_i, T_j^m is the melting point and $\Delta H_j^{s \rightarrow l}$ is the enthalpy of fusion of the solvent j. The value of $\Delta T/X_{Cu}^l$ as calculated from Eq 13, based on T_{Th}^m = 2031 K, $\Delta H_{Th}^{s \rightarrow l}$ = 13807 J/mol (11) and R=8.314 J/mol. K is -24.8 K/at.% Cu, as compared to -12 ± 2 K/at.% Cu, obtained from the liquidus proposed by Schiltz et al. (10). The corresponding value of $\Delta T/X_{Th}^l$ for T_{Cu}^m = 1358 K, $\Delta H_{Cu}^{s \rightarrow l}$ = 13054 J/mol is -11.8 K/at.% Th, which is slightly lower than that obtained from the experimental liquidus (10). Therefore, the (Cu) liquidus was modified to be compatible with the van't Hoff limiting slope, by imposing an additional small negative curvature to the existing liquidus. This resulted in slight alterations in the compositions of the liquidus used in the calculation. As for the Th-end of the

liquidus, only the data point at 1000°C eutectic temperature was used from Schiltz et al. (10). Two other liquidus data in the dilute range (<1 at.% Cu), that were estimated to be consistent with the limiting slopes according to Eq 13, were also used, along with other liquidus data from the Cu end, to model the enthalpy and entropy of the binary liquid. Approximation of the liquid by a subregular solution model was found to be adequate to reproduce the phase diagram satisfactorily. The resultant expression for the $^{E}_{\Delta G}{}^{l}$ was as follows (9):

$$^{E}_{\Delta G}{}^{l} = X(1-X)(-94200 + 50050\,X) \qquad \text{(J/mol)} \qquad (14)$$

where, X is the atomic fraction of Th.

The Gibbs energy of the Cu_6Th phase, expressed in the form (A + BT), was estimated next from the least squares fit of the phase equilibria data of this phase with the liquid at temperatures 935, 1055 and 1020°C, corresponding to liquid compositions 7, 14.29 and 18 at.% Th, respectively. For these calculations, Cu_6Th was assumed to be a line compound. In a similar manner, Gibbs energies for $Cu_{3.6}Th$, Cu_2Th and $CuTh_2$ were estimated from least squares fitting of the liquidus data at following temperatures.

$Cu_{3.6}Th$: 1020, 1052 and 980°C,
Cu_2Th : 980, 1015 and 880°C,
$CuTh_2$: 880, 1007 and 1000°C.

The Gibbs energy expressions for these phases, relative to pure liquid Cu and pure liquid Th as standard states are presented in Table I. For comparison with the measured data of Bailey et al. (8), the calculated ΔH values were normalized relative to pure solid Cu and pure solid Th (a Th) as standard states. As shown in Table II, the calculated ΔH values agree to within 2 to 20% of the measured values at 973 K, except for that of $Cu_{3.6}Th$. The reason for the large discrepency in the latter case is not clear.

The liquidus calculated at selected temperatures, based on the modeling parameters in Table I, is shown by "+" marks in Fig 2. Since the results fall on the experimental boundaries, our modeling appears to be self-consistent. Also shown in Fig. 2 is the calculated liquidus in equilibrium with both (aTh) and (ßTh). The liquid composition at the (ßTh) -> (aTh) transition temperature assumed to be at 1363°C (2) is approximately 83.8 at.% Th.

Table I. Thermodynamic Parameters in Cu-Th System*

Lattice stability parameters (a)

$^{o}G^{L}_{Cu} = 0$

$^{o}G^{L}_{Sr} = 0$

$^{o}G^{(Cu)}_{Cu} = -13054 + 9.613\,T$

$^{o}G^{(\beta Th)}_{Th} = -13807 + 6.80\,T \pm 1255$

$^{o}G^{(\alpha Th)}_{Th} = -17405 + 9.00\,T$

$(^{o}G^{\alpha Th \rightarrow \beta Th} = 3600 - 2.20\,T \pm 120)$

Integral Molar Gibbs Energies (b)

$G^{L} = X(1-X)(-94200 + 50050\,X) + RT[X \ln X + (1-X)\ln(1-X)]$

where X is atomic fraction of Th.

$G^{Cu_6Th} = -22065 + 5.20\,T$

$G^{Cu_{3.6}Th} = -18600 - 1.04\,T$

$G^{Cu_2Th} = -40075 + 12.425\,T$

$G^{CuTh_2} = -39400 + 14.955\,T$

where mol for the compounds refer to an atom as the elementary entity.

Standard States: pure liquid Cu and pure liquid Th.

---

* All units are in J/mol.

(a) From Hultgren et al. (2). (b) From phase diagram (9).

Table II. Thermodynamic Properties of Cu-Th Compounds at 973 K*

Parameters	Cu_6Th	$Cu_{3.6}Th$	Cu_2Th	$CuTh_2$	Reference
$-\Delta G$	13.68 ± 0.04	20.88 ± 0.08	26.36 ± 0.17	26.78 ± 0.21	(8)
$-\Delta G$	12.60	14.84	22.64	17.85	(9)
$-\Delta H$	10.46 ± 0.50	17.24 ± 0.67	25.98 ± 1.46	27.24 ± 0.21	(8)
$-\Delta H$	8.40	4.60	25.57	23.45	(9)

* All units are in J/mol.
Standard States: Pure solid Cu and pure solid Th.

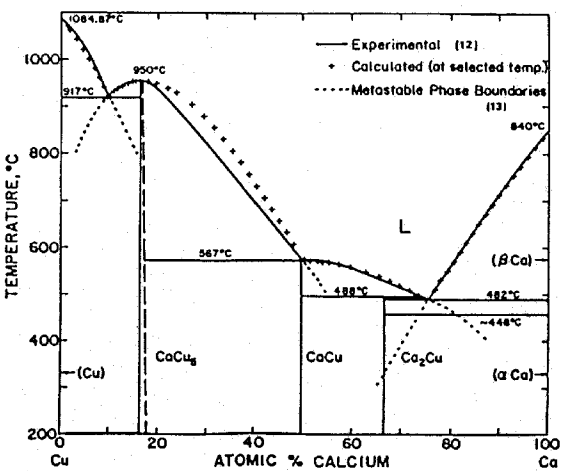

Figure 3 - The Copper-Calcium Phase Diagram.
The accepted boundaries are based on experimental data (12). Cu and Ca show negligible, mutual solid solubility. Calculated results show both stable and metastable boundaries (13).

The Cu-Ca equilibrium diagram is shown in Fig. 3 (12,13). The (Cu) liquidus between 1084.87 and 917°C, and the (Ca) liquidus between 840 and 482°C, respectively, were utilized to derive the parameters for the liquid, applying Eqs 6 and 7, as described for the Cu-Th system. A total of 35 data points were used to derive two coefficients for a_i and one for b_j that could reproduce the phase diagram satisfactorily. The resultant expression for the excess Gibbs energy of the liquid, $^{E}\Delta G^{l}$, is as follows:

$$^{E}\Delta G^{l} = X(1-X)(-26480 + 12550X - 12.28\,T) \qquad (J/mol) \qquad (15)$$

where, X is the atomic fraction of Ca. The validity of Eq 15 was checked against the only reported experimental data for the Gibbs energy of the liquid of Cu-26 at.% Ca at 1150 K (14). This value, when normalized relative to pure liquid Cu and pure liquid Ca as standard states used in our computation, agreed to within 5% of the value calculated from Eq 15 (-12100 J/mol vs. -12700 J/mol, respectively).

These two cases show that the modeling parameters obtained from the phase diagram can be in good agreement with experimentally determined thermodynamic data.

Case C

The recently assessed Cu-Sr equilibrium diagram is shown in Fig. 4 (15). The phase boundaries shown by solid lines are based on the works of Bruzzone (12). No thermodynamic data exist either for the two stoichiometric compounds, Cu_5Sr and CuSr, or for the liquid. The two terminal phases based on Cu and Sr, respectively, have negligible solubility fields, so that their thermodynamic properties are described adequately by those for the respective elements. Following the same procedure as outlined previously for the Cu-Th and Cu-Ca systems, interaction parameters for the liquid were modeled from the phase equilibria between the liquidus and the two terminal solid solution phases. The Gibbs energy expressions for Cu_5Sr and CuSr were also modeled from the phase diagram, and the combined results are presented in Table III. Self-consistency for the parameters so derived was checked by calculating the liquidus values at selected temperatures, and are shown by "+" symbols in Fig. 4. In addition, the relative stability of Cu_5Sr and CuSr, with respect to (Cu) and (Sr) phases at lower temperatures was examined, by considering the relative changes with temperature of Gibbs energies of the four phases. The calculations indicated that the Cu_5Sr phase decomposes at about -28°C into (Cu) and CuSr phases. The resultant

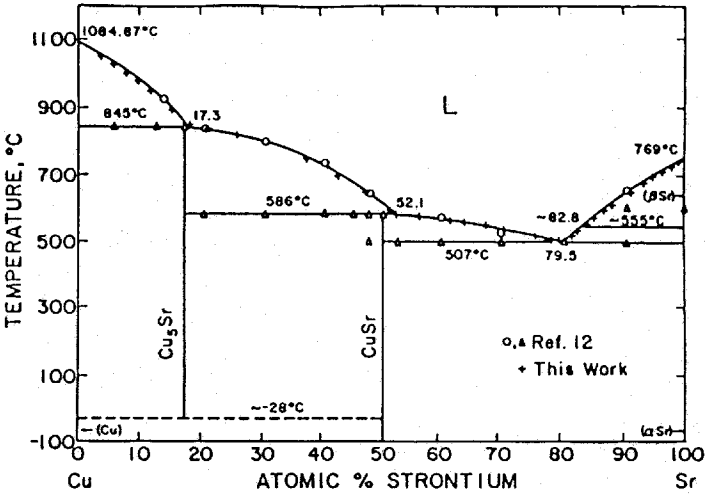

Figure 4 - The Copper-Strontium Phase Diagram.
The eutectoid transformation at -28°C and the liquid composition at ~82.8 at.% Sr are derived from modeling analysis(15).

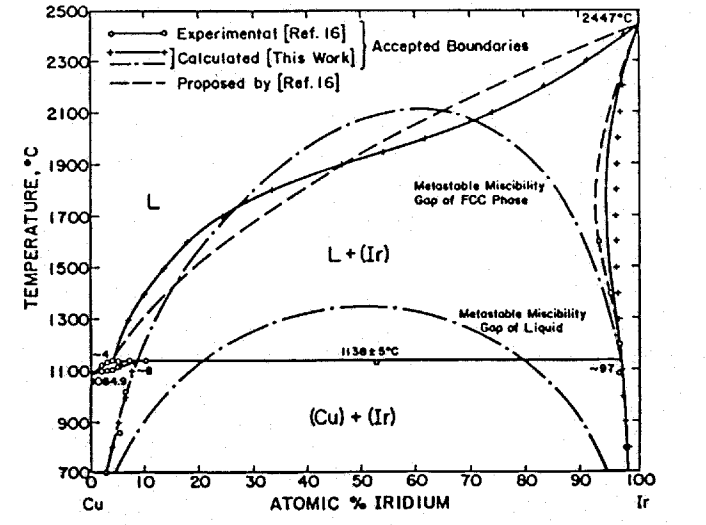

Figure 5 - The Copper-Iridium Phase Diagram.
The liquidus and solidus above the peritectic temperature, and the metastable miscibility gap boundaries are derived from thermodynamic calculation (17).

Table III. Thermodynamic Properties of Phases in Cu-Sr System*

Lattice stability parameters (a)

$^{0}G^{L}_{Cu} = 0$

$^{0}G^{L}_{Sr} = 0$

$^{0}G^{(Cu)}_{Cu} = -13054 + 9.613\,T$

$^{0}G^{(\beta Sr)}_{Sr} = -8276 + 7.95\,T$

$^{0}G^{(\alpha Sr)}_{Sr} = -9075 + 8.92\,T$

$(\,^{0}G^{\alpha Sr \rightarrow \beta Sr} = 799 - 0.97\,T)$

Integral Molar Gibbs Energies (b)

$G^{L} = X(1-X)(-20780 + 7.55\,T) + RT[X \ln X + (1-X)\ln(1-X)]$

where X is atomic fraction of Sr.

$G^{Cu_5Sr} = -18995 + 11.70\,T$

$G^{CuSr} = -34350 + 30.10\,T$

where mol for Cu_5Sr and CuSr refers to an atom as the elementary entity.

Standard States: pure liquid Cu and pure liquid Sr.

---

*All units are in J/mol.

(a) From Hultgren et al. (2). (b) From phase diagram (15).

eutectoid transformation is indicated in Fig. 4 by a dotted line, giving an example of the additional information that the modeling generated.

Case D

The Cu-Ir equilibrium diagram has been determined experimentally only in part (16), while most of the liquidus and the Ir-rich solidus that extend to very high temperatures are not known. In our modeling (17), the interaction parameters for the (Cu) and (Ir) phases were assumed to be identical, since they both have the fcc structure. These were determined from the known phase equilibria data existing between 700^0 and the peritectic temperature at 1138^{0}C, see Fig. 5. Next , the phase equilibria at 1138^{0}C, where the liquid of 4 at.% Ir coexists with (Cu) of about 8 at.% and (Ir) of 97 at.% Ir, were utilized to derive the interaction parameter for the liquid. In the present instance, the fcc phase was approximated by a subregular solution, while the liquid was modeled to a regular solution due to the lack of sufficient data. The results are shown in Table IV. Using these parameters, the liquidus and the Ir-rich solidus were calculated. The latter shows a retrograde behavior, and compares well with the limited experimental solidus data available up to 1600^{0}C. The thermodynamic consistency between the calculated liquidus and solidus was checked by comparing the partition coefficient, K, estimated from Fig. 5 at dilute ranges near the Ir-end, with the calculated value obtained from the van't Hoff's relation given below :

$$X_{Cu}^{(Ir)} / X_{Cu}^{l} = 1 + [\Delta H_{Ir}^{s \rightarrow l} / R(T_{Ir}^{m})^2] . (\Delta T / X_{Cu}^{l}) \qquad (16)$$

The value of K as obtained from Fig. 5 is approximately 0.28 ± 0.01 and compares very well with the theoretical value of 0.29 ± 0.02 obtained from Eq 16, using the initial slope of the liquidus (1667^{0}C / at.% Cu) from Fig. 5. Thus, our calculated liquidus and solidus boundaries for (Ir) appear to be consistent both thermodynamically, and with the limited experimental data available. The corresponding values of K derived from the proposed (interpolated) liquidus of Raub and Roeschel (16) are, respectively, 0.25 and 0.62 ± 0.03. This indicates a discrepency with the van't Hoff's relation.

The calculated liquidus in Fig. 5 shows an inflection point, which indicates the likelihood of a miscibility gap developing at lower temperatures. The metastable gap of the liquid, as well as that for the fcc phase, were calculated by suppressing the stability of the coexisting equilibrium phases and are shown superimposed on the stable boundaries in

Table IV. Thermodynamic Parameters in Cu-Ir System*

Lattice stability parameters (a)

$^{o}G^{L}_{Cu} = 0$

$^{o}G^{L}_{Ir} = 0$

$^{o}G^{(Cu)}_{Cu} = -13054 + 9.613\,T$

$^{o}G^{(Ir)}_{Ir} = -26137 + 9.609\,T$

Integral Molar Excess Gibbs Energies (b)

$G^{L} = X(1-X)(26990)$

$G^{fcc} = X(1-X)(32980 + 10360\,X)$

where X is atomic fraction of Ir.

Standard States: pure liquid Cu and pure liquid Ir.

* All units are in J/mol.
(a) From Hultgren et al. (2). (b) From phase diagram (17).

Fig. 5. The symmetric gap for the liquid is a consequence of the regular solution approximation. A much higher miscibility gap for the fcc phase suggests, that it is more difficult to form a metastable, single phase fcc solid solution between Cu and Ir, and requires a much higher temperature (>~2100°C) than that (>~1300°C) for a metastable single phase liquid solution. It is interesting to note, that the location of the miscibility gap has direct bearing on the slope of the corresponding stable boundary of the same phase. Thus, as the peak of the miscibility gap for the liquid moves closer to the liquidus, the slope of the latter becomes progressively shallower, and ultimately becomes essentially horizontal, as the gap touches it, as in the case of Cu-Cr system in Fig. 1 (7).

Thus the above example shows how undetermined phase boundaries, including the metastable ones, could be estimated from the modeling of known regions of the phase diagram.

Summary and Conclusions

Using examples drawn from our evaluations of various copper binary alloy systems we have demonstrated several important uses of thermodynamic modeling in the evaluation of binary phase diagrams. The cases presented herein showed that some controversies can be resolved, and experimentally unattainable portions of the diagram could be calculated. Furthermore, in some cases the thermodynamic parameters derived from the phase diagram are in good agreement with experimentally determined ones. It is believed that the straight forward techniques described herein should be applicable to many systems when sufficient information is available. This would enhance the evaluations in that the phase diagram data could be checked for consistency with fundamental thermodynamic relations.

Acknowledgements

We wish to thank our many colleagues in the binary evaluation program for many useful interactions. In particular, we thank Professor A. D. Pelton, Drs. J. Murray and H. Okamoto for stimulating discussions. Part of our calculations were performed using the computer programs of Mr. E. S. K. Menon, based on some of the equations presented in this paper. The continued financial support of INCRA and the OSRD of NBS is gratefully acknowledged.

References

1. M. Hansen and K. Anderko, Constitution of Binary Alloys, 2nd ed., McGraw-Hill Inc., New York, NY, 1958.
2. R. Hultgren, P.D. Desai, D. T. Hawkins, M. Gleiser, K. K. Kelley, and D. D. Wagman, Selected Values of the Thermodynamic Properties of the Elements, ASM, Metals Park, OH, 1973.
3. G. Hindrichs, " Some Cr and Mn Alloys", Z. Anorg. Chem., 5(1908) pp. 420-423.
4. E. Siedschlag, "Cr-Cu-Ni Alloys", Z. Anorg. Chem., 131 (1923) pp. 173-178.
5. G. M. Kuznetsov, V. N. Fedorov and A. L. Rodnyanskaya, "Investigation of Phase Diagrams of Cu-Cr System", Sov. Non-Ferrous Met. Res., 3 (1977) pp. 104-105.
6. L. Timberg and J. M. Toguri, "A Thermodynamic Study of (Copper + Chromium) by Mass Spectrometry", J. Chem. Thermodyn., 14(1982) pp. 193-199.
7. D. J. Chakrabarti and D. E. Laughlin, "The Chromium-Copper System",

Bull. Alloy Phase Diagrams, 5(1) (1984) pp. 59-68.
8. D. M. Bailey and J. F. Smith, "Thermodynamics of Formation of Th-Cu Alloys", IAEA-SM-190/47, Conf. 741030-43, 1974.
9. D. J. Chakrabarti, D. E. Laughlin and D. E. Peterson, "The Copper-Thorium System", To be published in Bull. Alloy Phase Diagrams.
10. R. J. Schiltz, E. R. Stevens and O. N. Carlson, "The Th-Cu System", J. Less Common Met., 25 (1971) pp.175-185.
11. L. S. Levinson, "Heat Content of Crystal Bar Th", J. Nucl. Mater., 19 (1966) pp. 50-52.
12. G. Bruzzone, "Binary Systems of Ca-Cu, Sr-Cu and Ba-Cu", J. Less Common Met., 25 (1971) pp. 361-366.
13. D. J. Chakrabarti and D. E. Laughlin, "The Calcium-Copper System", Bull. Alloy Phase Diagrams, 5(6) (1984) pp. 570-576.
14. M. Notin, C. Cunat and J. Hertz, "Electrochemical Determination of Thermodynamic Properties of Formation of Binary Alloys (Ca, Cu) between 800 and 1300 K using Cells with Solid CaF_2 Electrolyte", Thermochim. Acta, 33 (1979) pp.175-185.
15. D. J. Chakrabarti and D. E. Laughlin, "The Copper-Strontium System", Bull. Alloy Phase Diagrams, 5(4) (1984) pp. 391-396.
16. E. Raub and E. Roeschel, "Copper-Iridium Alloys", Z. Metallkunde, 60 (1969) pp.142-144.
17. D. J. Chakrabarti and D. E. Laughlin, "The Copper-Iridium System", To be published in Bull. Alloy Phase Diagrams.